Journal of Computational Science and Technology

Vol. 3, No. 1, 2009

Stress Intensity Factor for a Planar Interfacial Crack in Three Dimensional Bimaterials*

Nao-Aki NODA**, Chunhui XU*** and Yasushi TAKASE****

** Department of Mechanical Engineering, Kyushu Institute of Technology
Sensui-Cho 1-1 Tobata-Ku, Kitakyushu-Shi, Fukuoka, Japan
E-mail: noda@mech.kyutech.ac.jp
*** College of Science, China Agricultural University, Beijing 100083, P.R.CHINA
E-mail:xuchunhui_cau@163.com
**** Department of mechanical Engineering, Kyushu Institute of Technology
Sensui-Cho 1-1 Tobata-Ku, Kitakyushu-Shi, Fukuoka, Japan
E-mail: takase@mech.kyutech.ac.jp

Abstract

In this paper, stress intensity factors for a three dimensional planar interfacial crack are considered on the idea of the body force method. The formulation leads to a system of singular integral equation, whose unknowns are three types of crack opening displacements. The unknown body force densities are approximated by the products of the fundamental density functions and power series; here, the fundamental density functions are chosen to express singular stress fields due to a two-dimensional interface crack exactly. The calculation shows that the present method gives rapidly converging numerical solutions. It is found that the stress intensity factors K_I and K_{II} are determined by bimaterials constant ε alone, independent of elastic modulus ratio and Poisson's ratio.

Key words: Elasticity, Stress Intensity Factor, Body Force Method, Interface Crack, Fracture Mechanics, Composite Material, Singular Integral Equation

1. Introduction

Composite structures and adhesive or bonded joints are widely used in recent electronic and mechanical products including a lot of interfaces. Failures of those products are dominated by interfacial destruction because they usually originate from the interfacial region. From this aspect, the accurate evaluation of interface cracks in dissimilar materials has been important. Previously, two-dimensional interfacial crack problems were analyzed by Salganik [1] and many other researchers [2]-[9]. Also, several important three-dimensional interfacial crack problems were treated by some researchers for a penny-shaped interfacial crack [10]-[15], an elliptical crack [16], and a crack in a finite body [17]; however, usually they are considered under specific material combinations. In other words, closed form solutions of stress intensity factors (SIFs) are only available for a penny shaped interfacial crack [17], and a deep external interfacial crack [18] under any combination of materials.

Considering these situations, in our previous paper [19], an axi-symmetric ring-shaped interfacial crack was analyzed under tension and torsion load using the body force method. Here, the unknown functions of singular integral equations in this method were approximated by the products of the fundamental density functions and power series [19]-[22]. Then, it was found that accurate smooth distributions of SIFs along crack front in 3-D homogenous materials are obtained. However, more general 3-D interfacial crack

*Received 19 Dec., 2008 (No. T1-06-0860)
Japanese Original : Trans. Jpn. Soc. Mech. Eng., Vol.73, No.727, A (2007), pp.379-386 (Received 21 Aug., 2006)
[DOI: 10.1299/jcst.3.212]

problems have not been covered yet until now. Chen-Noda-Tang [23] has given the general expressions of the singular integral equations for 3-D interfacial crack problems. However, it is difficult to solve these equations accurately considering the stress oscillation singularity and overlapping of crack surface, which are peculiar to interfacial cracks.

In this paper, therefore, accurate numerical solutions will be considered for rectangular interfacial crack, and the stress intensity factors will be discussed on the basis of the results. In the numerical solution, the fundamental density functions are chosen to express the singular stress fields for rectangular crack. The stress intensity factors will be given from the value of unknown functions directly in this numerical procedure.

2. Hypersingular intergro-differential equations for 3D bimaterial interfacial crack problems

Figure 1 (a) shows the problem figuration of the interfacial crack in a bimaterial. As shown in Eq (1), the hypersingular intergro-differential equations for this interfacial crack problem were derived by Chen-Noda-Tang [23], whose unknown functions are crack opening displacements u_x, u_y, u_z. Here, (x, y, z) is a coordinate in question, and (ξ, η, ζ) is a point where body force is applied. The notations p_x, p_y, p_z denote surface tractions, μ_1, μ_2 are the shear modulus, ν_1, ν_2 are the Poisson ratios.

$$\mu_1\left(\Lambda_2-\Lambda_1\right)\frac{\partial \Delta u_z\left(x,y\right)}{\partial x}+\mu_1\frac{\left(2\Lambda-\Lambda_1-\Lambda_2\right)}{2\pi}⨎_s\frac{1}{r^3}\Delta u_x(\xi,\eta)dS(\xi,\eta)$$
$$+3\mu_1\frac{\left(\Lambda_1+\Lambda_2-\Lambda\right)}{2\pi}\left\{⨎_s\frac{\left(x-\xi\right)^2}{r^5}\Delta u_x(\xi,\eta)dS(\xi,\eta)+⨎_s\frac{\left(x-\xi\right)\left(y-\eta\right)}{r^5}\Delta u_y(\xi,\eta)dS(\xi,\eta)\right\}=-p_x(x,y) \tag{1a}$$

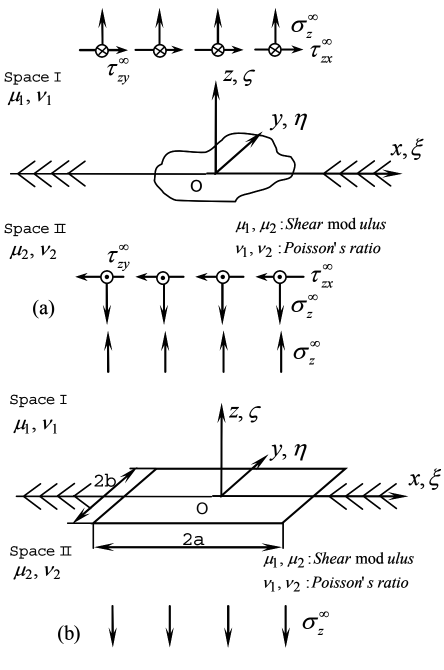

Fig.1 Problem configuration

$$\mu_1\left(\Lambda_2-\Lambda_1\right)\frac{\partial\Delta u_z\left(x,y\right)}{\partial y}+\mu_1\frac{\left(2\Lambda-\Lambda_1-\Lambda_2\right)}{2\pi}\oint_s\frac{1}{r^3}\Delta u_y(\xi,\eta)dS(\xi,\eta)$$
$$+3\mu_1\frac{\left(\Lambda_1+\Lambda_2-\Lambda\right)}{2\pi}\left\{\oint_s\frac{(x-\xi)(y-\eta)}{r^5}\Delta u_x(\xi,\eta)dS(\xi,\eta)+\oint_s\frac{(y-\eta)^2}{r^5}\Delta u_y(\xi,\eta)dS(\xi,\eta)\right\}=-p_y(x,y)$$

(1b)

$$\mu_1\left(\Lambda_1-\Lambda_2\right)\left(\frac{\partial\Delta u_x\left(x,y\right)}{\partial x}+\frac{\partial\Delta u_y\left(x,y\right)}{\partial y}\right)+\mu_1\frac{\left(\Lambda_1+\Lambda_2\right)}{2\pi}\oint_s\frac{1}{r^3}\Delta u_z(\xi,\eta)dS(\xi,\eta)=-p_z\left(x,y\right) \quad (1c)$$

$\left(x,y\right)\in S$,

$$\Lambda=\frac{\mu_2}{\mu_1+\mu_2},\quad \Lambda_1=\frac{\mu_2}{\mu_1+\kappa_1\mu_2},\quad \Lambda_2=\frac{\mu_2}{\mu_2+\kappa_2\mu_1},$$
$$\kappa_1=3-4\nu_1,\quad \kappa_2=3-4\nu_2,\quad r^2=\left(x-\xi\right)^2+\left(y-\eta\right)^2$$

(1d)

$$\Delta u_i\left(x,y\right)=u_i(x,y,0^+)-u_i(x,y,0^-),(i=x,y,z) \quad (1e)$$

The integration $\oint_S$ should be interpreted in a sense of a finite part integral in the cracked region S.

3. Method of analysis

To determine three unknown functions in Eq (1), it is essential to choose fundamental densities functions, which express particular singular stress fields of interface crack. From this aspect, two-dimensional solutions for 2D crack problem will be considered again. Figure 2 shows an interface crack with a length of 2a in an infinity bimaterial under normal stress σ_0 and shear stress τ_0 at the infinity. Three types of crack opening displacements $\Delta u_x,\Delta u_y,\Delta u_z$ are given by Rice-Sih [4]. They are equivalent to body force densities $w_x(\xi)$, $w_y(\xi)$, $w_z(\xi)$ as shown in the following equations.

For Fig. 2(a):

$$\Delta u_z+i\Delta u_x=\sum_{l=1}^{2}\left\{\frac{\kappa_l-1}{\mu_l(1+\kappa_l)}w_z(\xi)+i\frac{1}{\mu_l}w_x(\xi)\right\}\times\left[\sigma_0+i\tau_0\right]$$
$$=\sum_{l=1}^{2}\frac{1+\kappa_l}{4\mu_l\cosh\pi\varepsilon}\sqrt{a^2-\xi^2}\left(\frac{a-\xi}{a+\xi}\right)^{i\varepsilon}\times\left[\sigma_0+i\tau_0\right], \quad (2)$$

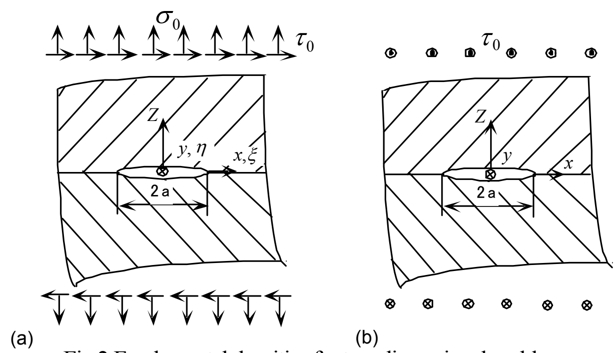

Fig.2 Fundamental densities for two dimensional problems

For Fig. 2(b):

$$\Delta u_y = \sum_{l=1}^{2} \frac{1}{\mu_l} w_y(\xi)\tau_0 = \sum_{l=1}^{2} \frac{1}{\mu_l} \frac{1+\kappa_l}{4} \sqrt{a^2-\xi^2}\,\tau_0 \tag{3}$$

Here, σ_0, τ_0 are the tensile stress and shear stress applied at infinity, ε and κ are defined as follows:

$$\varepsilon = \frac{1}{2\pi}\ln\left(\frac{\mu_2\kappa_1+\mu_1}{\mu_1\kappa_2+\mu_2}\right), \quad \kappa_l = \begin{cases} \dfrac{3-\nu_l}{1+\nu_l} & \text{plane stress} \\ 3-4\nu_l & \text{plane strain} \end{cases} \tag{4}$$

Considering the Eqs. (2) and (3) available for 2D interfacial crack problem, the following expressions will be used for a rectangular interfacial crack shown in Fig.1 (b).

$$\Delta u_i\left(\xi,\eta\right) = w_i(\xi,\eta)F_i(\xi,\eta), i = x, y, z \tag{5}$$

Here, $w_i(\xi,\eta)$ is defined as follows:

$$\left.\begin{aligned} w_x(\xi,\eta) &= \sum_{l=1}^{2} \frac{1+k_l}{4\mu_l \cosh \pi\varepsilon} \sqrt{a^2-\xi^2}\sqrt{b^2-\eta^2}\, \sin\left(\varepsilon \ln\left(\frac{a-\xi}{a+\xi}\right)\right) \\ w_y(\xi,\eta) &= \sum_{l=1}^{2} \frac{1+k_l}{4\mu_l \cosh \pi\varepsilon} \sqrt{a^2-\xi^2}\sqrt{b^2-\eta^2}\, \sin\left(\varepsilon \ln\left(\frac{b-\eta}{b+\eta}\right)\right) \\ w_z(\xi,\eta) &= \sum_{l=1}^{2} \frac{1+k_l}{4\mu_l \cosh \pi\varepsilon} \sqrt{a^2-\xi^2}\sqrt{b^2-\eta^2}\, \cos\left(\varepsilon \ln\left(\frac{a-\xi}{a+\xi}\right)\right)\cos\left(\varepsilon \ln\left(\frac{b-\eta}{b+\eta}\right)\right) \end{aligned}\right\} \tag{6}$$

To approximate unknown functions as continuous functions, the following polynomial forms will be used for $F_x(\xi,\eta), F_y(\xi,\eta), F_z(\xi,\eta)$.

$$\begin{aligned} F_x(\xi,\eta) &= \alpha_0 + \alpha_1\eta + \cdots + \alpha_{n-1}\eta^{(n-1)} + \alpha_n\eta^n + \alpha_{n+1}\xi + \alpha_{n+2}\xi\eta + \cdots + \alpha_{2n}\xi\eta^n + \cdots \\ &\quad + \alpha_{l-n-1}\xi^m + \alpha_{l-n}\xi^m\eta + \cdots + \alpha_{l-1}\xi^m\eta^n = \sum_{i=0}^{l-1}\alpha_i G_i(\xi,\eta), \\ F_y(\xi,\eta) &= \beta_0 + \beta_1\eta + \cdots + \beta_{n-1}\eta^{(n-1)} + \beta_n\eta^n + \beta_{n+1}\xi + \beta_{n+2}\xi\eta + \cdots + \beta_{2n}\xi\eta^n + \cdots \\ &\quad + \beta_{l-n-1}\xi^m + \beta_{l-n}\xi^m\eta + \cdots + \beta_{l-1}\xi^m\eta^n = \sum_{i=0}^{l-1}\beta_i G_i(\xi,\eta), \\ F_z(\xi,\eta) &= \gamma_0 + \gamma_1\eta + \cdots + \gamma_{n-1}\eta^{(n-1)} + \gamma_n\eta^n + \gamma_{n+1}\xi + \gamma_{n+2}\xi\eta + \cdots + \gamma_{2n}\xi\eta^n + \cdots \\ &\quad + \gamma_{l-n-1}\xi^m + \gamma_{l-n}\xi^m\eta + \cdots + \gamma_{l-1}\xi^m\eta^n = \sum_{i=0}^{l-1}\gamma_i G_i(\xi,\eta), \end{aligned} \tag{7}$$

$$l = \left(m+1\right)\left(n+1\right),$$

$$G_0\left(\xi,\eta\right) = 1,\ G_1\left(\xi,\eta\right) = \eta,\ \cdots, G_{n+1}\left(\xi,\eta\right) = \xi,\ \cdots, G_{l-1}\left(\xi,\eta\right) = \xi^m\eta^n.$$

Using the approximation method mentioned above, we obtain the following system of linear equations for the determination of the coefficients $\alpha_i, \beta_i, \gamma_i$. The unknown coefficients $\alpha_i, \beta_i, \gamma_i$, whose number is 3l, are then determined from (8) by selecting a set of collocation points to minimize the residual stresses.

$$\left.\begin{aligned}
&\sum_{i=0}^{l-1}\alpha_i(f_{x1}^1+f_{x1}^2)+\sum_{i=0}^{l-1}\beta_i f_{y1}+\sum_{i=0}^{l-1}\gamma_i f_{z1}=-p_x\\
&\sum_{i=0}^{l-1}\alpha_i f_{x2}+\sum_{i=0}^{l-1}\beta_i(f_{y2}^1+f_{y2}^2)+\sum_{i=0}^{l-1}\gamma_i f_{z2}=-p_y\\
&\sum_{i=0}^{l-1}\alpha_i f_{x3}+\sum_{i=0}^{l-1}\beta_i f_{y3}+\sum_{i=0}^{l-1}\gamma_i f_{z3}=-p_z
\end{aligned}\right\} \tag{8}$$

Where,

$$f_{z1}=\mu_1(\Lambda_2-\Lambda_1)\sum_{l=1}^{2}\frac{1+k_l}{4\mu_l\cosh\pi\varepsilon}\times\frac{1}{\sqrt{a^2-x^2}}\times x^{-1+m}y^n\sqrt{b^2-y^2}\left(\cos\varepsilon\ln(\frac{b-y}{b+y})\right)$$
$$\times\left[\left(a^2m-(1+m)x^2\right)\times\cos\left(\varepsilon\ln\left(\frac{a-x}{a+x}\right)\right)+2a\varepsilon x\sin\left(\varepsilon\ln(\frac{a-x}{a+x})\right)\right] \tag{9a}$$

$$f_{z2}=\mu_1(\Lambda_2-\Lambda_1)\sum_{l=1}^{2}\frac{1+k_l}{4\mu_l\cosh\pi\varepsilon}\times\frac{1}{\sqrt{b^2-y^2}}\times y^{-1+n}x^m\sqrt{a^2-x^2}\left(\cos\varepsilon\ln(\frac{a-x}{a+x})\right)$$
$$\times\left[\left(b^2n-(1+n)y^2\right)\times\cos\left(\varepsilon\ln\left(\frac{b-y}{b+y}\right)\right)+2b\varepsilon y\sin\left(\varepsilon\ln(\frac{b-y}{b+y})\right)\right] \tag{9b}$$

$$f_{x3}=\mu_1(\Lambda_2-\Lambda_1)\sum_{l=1}^{2}\frac{1+k_l}{4\mu_l\cosh\pi\varepsilon}\times\frac{1}{\sqrt{a^2-x^2}}\times x^{-1+m}y^n\sqrt{b^2-y^2}$$
$$\times\left[\left(a^2m-(1+m)x^2\right)\times\sin\left(\varepsilon\ln\left(\frac{a-x}{a+x}\right)\right)-2a\varepsilon x\cos\left(\varepsilon\ln(\frac{a-x}{a+x})\right)\right] \tag{9c}$$

$$f_{y3}=\mu_1(\Lambda_2-\Lambda_1)\sum_{l=1}^{2}\frac{1+k_l}{4\mu_l\cosh\pi\varepsilon}\times\frac{1}{\sqrt{b^2-y^2}}\times y^{-1+n}x^m\sqrt{a^2-x^2}$$
$$\times\left[\left(b^2n-(1+n)y^2\right)\times\sin\left(\varepsilon\ln\left(\frac{b-y}{b+y}\right)\right)-2b\varepsilon y\cos\left(\varepsilon\ln(\frac{b-y}{b+y})\right)\right] \tag{9d}$$

$$f_{x1}^1=\mu_1\frac{2\Lambda-\Lambda_1-\Lambda_2}{2\pi}\oint_s\frac{1}{r^3}w_x(\xi,\eta)G_j(\xi,\eta)ds(\xi,\eta) \tag{9e}$$

$$f_{x1}^2=3\mu_1\frac{\Lambda_1+\Lambda_2-\Lambda}{2\pi}\oint_s\frac{(x-\xi)^2}{r^5}w_x(\xi,\eta)G_j(\xi,\eta)ds(\xi,\eta) \tag{9f}$$

$$f_{y1}=3\mu_1\frac{\Lambda_1+\Lambda_2-\Lambda}{2\pi}\oint_s\frac{(x-\xi)(y-\eta)}{r^5}w_y(\xi,\eta)G_j(\xi,\eta)ds(\xi,\eta) \tag{9g}$$

$$f_{y2}^1=\mu_1\frac{2\Lambda-\Lambda_1-\Lambda_2}{2\pi}\oint_s\frac{1}{r^3}w_y(\xi,\eta)G_j(\xi,\eta)ds(\xi,\eta) \tag{9h}$$

$$f_{x2}=3\mu_1\frac{\Lambda_1+\Lambda_2-\Lambda}{2\pi}\oint_s\frac{(x-\xi)(y-\eta)}{r^5}w_x(\xi,\eta)G_j(\xi,\eta)ds(\xi,\eta) \tag{9i}$$

$$f_{y2}^2=3\mu_1\frac{\Lambda_1+\Lambda_2-\Lambda}{2\pi}\oint_s\frac{(y-\eta)^2}{r^5}w_y(\xi,\eta)G_j(\xi,\eta)ds(\xi,\eta) \tag{9j}$$

$$f_{z3} = \mu_1 \frac{\Lambda_1 + \Lambda_2}{2\pi} = \!\!\!\!\!\!\!\int_s \frac{1}{r^3} w_z(\xi,\eta) G_j(\xi,\eta) ds(\xi,\eta) \tag{9k}$$

4. How to evaluate the singular integral equations

Equations (9e)-(9k) include hypersingularities when the point in question (x, y) coincides with the point (ξ,η) where body force is applied; and therefore they cannot be evaluated in the present form.

Using the Taylor's expansion with the local polar system $\xi - x = r\cos\theta,\ \eta - y = r\sin\theta$ as shown in Fig.3, the following expressions are given, and they will be applied to evaluate the integral.

$$\sqrt{a^2-\xi^2} = P_0(x) - (\xi - x)P_1(x) - (\xi - x)^2 P_2(\xi, x) \tag{10a}$$

$$\sqrt{b^2-\eta^2} = Q_0(y) - (\eta - y)Q_1(y) - (\eta - y)^2 Q_2(\eta, y) \tag{10b}$$

Here

$$P_0(x) = \sqrt{a^2-x^2}, \qquad P_1(x) = \frac{x}{\sqrt{a^2-x^2}},$$

$$P_2(\xi,x) = \frac{\xi + x}{\sqrt{a^2-x^2}\left(\sqrt{a^2-\xi^2}+\sqrt{a^2-x^2}\right)} \times \frac{a^2}{\left(\xi\sqrt{a^2-x^2}+x\sqrt{a^2-\xi^2}\right)}$$

$$Q_0(x) = \sqrt{b^2-y^2} \qquad Q_1(y) = \frac{y}{\sqrt{b^2-y^2}}$$

$$Q_2(\eta,y) = \frac{\eta + y}{\sqrt{b^2-y^2}\left(\sqrt{b^2-\eta^2}+\sqrt{b^2-y^2}\right)} \times \frac{b^2}{\left(\eta\sqrt{b^2-y^2}+y\sqrt{b^2-\eta^2}\right)}$$

$$\begin{aligned}\xi^m &= x^m + m x^{m-1}(\xi - x) + \sum_{i=0}^{m-2}\left[(i+1)\xi^{(m-2-i)}x^i\right](\xi - x)^2 \\ &= b_0(x) + b_1(x)(\xi - x) + b_2(\xi, x)(\xi - x)^2\end{aligned} \tag{10c}$$

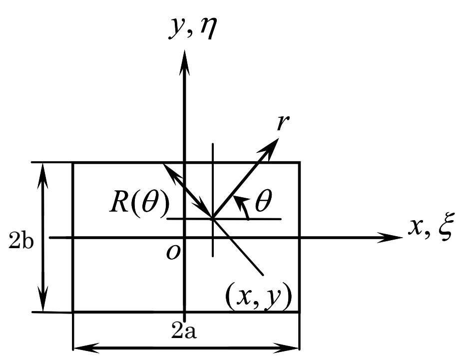

Fig.3 Integral parameter

$$\eta^n = x^n + nx^{n-1}(\eta - y) + \sum_{i=0}^{n-2}\left[(i+1)\eta^{(n-2-i)}y^i\right](\eta - y)^2 \\ = c_0(y) + c_1(y)(\eta - y) + c_2(\eta, y)(\eta - y)^2 \tag{10d}$$

$$FC_{11} = \cos\left(\varepsilon\ln(\frac{a-\xi}{a+\xi})\right) = R_{01}(x) + R_{11}(x)(\xi - x) + R_{21}(x)(\xi - x)^2 \tag{10e}$$

$$FS_{11} = \sin\left(\varepsilon\ln(\frac{a-\xi}{a+\xi})\right) = R_{02}(x) + R_{12}(x)(\xi - x) + R_{22}(x)(\xi - x)^2 \tag{10f}$$

$$FC_{21} = \cos\left(\varepsilon\ln(\frac{b-\eta}{b+\eta})\right) = T_{01}(y) + T_{11}(y)(\eta - y) + T_{21}(y)(\eta - y)^2 \tag{10g}$$

$$FS_{21} = \sin\left(\varepsilon\ln(\frac{b-\eta}{b+\eta})\right) = T_{02}(y) + T_{12}(y)(\eta - y) + T_{22}(y)(\eta - y)^2 \tag{10h}$$

Here

$$R_{01} = \cos\left(\varepsilon\ln(\frac{a-x}{a+x})\right), \quad R_{02} = \sin\left(\varepsilon\ln(\frac{a-x}{a+x})\right),$$

$$T_{01} = \cos\left(\varepsilon\ln(\frac{b-y}{b+y})\right), \quad T_{02} = \sin\left(\varepsilon\ln(\frac{b-y}{b+y})\right),$$

$$R_{11}(x) = \frac{2a\varepsilon}{a^2 - x^2}R_{02}, \quad R_{12}(x) = -\frac{2a\varepsilon}{a^2 - x^2}R_{01}, \quad T_{11}(y) = \frac{2b\varepsilon}{b^2 - y^2}T_{02},$$

$$T_{12}(y) = -\frac{2b\varepsilon}{b^2 - y^2}T_{01},$$

$$R_{21}(x) = \begin{cases} \dfrac{1}{(\xi - x)^2}\left(FC_{11} - R_{01}(x) - R_{11}(x)(\xi - x)\right) & |x - \xi| \ge \varepsilon_0 \\ \dfrac{2a\varepsilon x}{\left(a^2 - x^2\right)^2}R_{02} - \dfrac{2a^2\varepsilon^2}{\left(a^2 - x^2\right)^2}R_{01} & |x - \xi| \le \varepsilon_0 \end{cases},$$

$$R_{22}(x) = \begin{cases} \dfrac{1}{(\xi - x)^2}\left(FS_{11} - R_{02}(x) - R_{12}(x)(\xi - x)\right) & |x - \xi| \ge \varepsilon_0 \\ \dfrac{2a\varepsilon x}{\left(a^2 - x^2\right)^2}R_{01} - \dfrac{2a^2\varepsilon^2}{\left(a^2 - x^2\right)^2}R_{02} & |x - \xi| \le \varepsilon_0 \end{cases},$$

$$T_{21}(y) = \begin{cases} \dfrac{1}{(\eta - y)^2}\left(FC_{21} - T_{01}(y) - T_{11}(y)(\eta - y)\right) & |y - \eta| \ge \varepsilon_0 \\ \dfrac{2b\varepsilon y}{\left(b^2 - y^2\right)^2}T_{02} - \dfrac{2b^2\varepsilon^2}{\left(b^2 - y^2\right)^2}T_{01} & |y - \eta| \le \varepsilon_0 \end{cases},$$

$$T_{22}(y) = \begin{cases} \dfrac{1}{(\eta-y)^2}\left(FS_{21} - T_{02}(y) - T_{12}(y)(\eta-y)\right) & |y-\eta| \ge \varepsilon_0 \\ \dfrac{2b\varepsilon y}{\left(b^2-y^2\right)^2} T_{01} - \dfrac{2b^2\varepsilon^2}{\left(b^2-y^2\right)^2} T_{02} & |y-\eta| \le \varepsilon_0 \end{cases}.$$

In actual numerical calculation, we may put $\varepsilon_0 = 10^{-10}$. Using the concept of finite-part integral method with the relations (10), the hypersingular integrals in (9e)-(9k) can be reduced to the following form:

$$I_{mn}(x,y) = \int_0^{2\pi}\int_0^{R(\theta)}\left[\frac{D_0(x,y)}{r^2} + \frac{D_1(\theta)}{r}\right]drd\theta + \int_0^{2\pi}\int_0^{R(\theta)} D_2(r,\theta)drd\theta$$

$$= \int_0^{2\pi}\left[-\frac{D_0(x,y)}{R(\theta)} + D_1(x,y,\theta)\ln(R(\theta))\right]\mathrm{d}\theta + \int_0^{2\pi}\int_0^{R(\theta)} D_2(x,y,r,\theta)\mathrm{d}r\mathrm{d}\theta. \quad (11)$$

Here, the notation $R(\theta)$ means a distance between a point (x,y) in question and a point on the circumference of the crack as shown in Fig.3. In Eq. (11), $D_0(x,y)$, $D_1(x,y,\theta)$ and $D_2(x,y,r,\theta)$ are known functions, which can be expressed as a combination of the terms in Eq. (10). Using the expressions $I_{mn}(x,y)$ shown in Eq. (11), all integrals can be evaluated accurately by applying normal numerical integral procedure.

5. Numerical results and discussion

5.1 Definition of dimensionless stress intensity factors

According to the stress intensity factors of a 2D interfacial crack with length of 2b, the definition of dimensionless stress intensity factors F_I, F_{II} are defined as follows:

$$F_I + iF_{II} = \frac{K_I(x,y)\big|_{x=x,y=\pm b} + iK_{II}(x,y)\big|_{x=x,y=\pm b}}{\sigma_z^\infty\sqrt{\pi b}}$$

$$= \sqrt{a^2 - x^2} \times (\cos\left(\varepsilon \ln(\frac{a-x}{a+x})\right) F_z(x,y)\big|_{x=x,y=\pm b} + 2i\varepsilon F_y(x,y)\big|_{x=x,y=\pm b}), \quad (12a)$$

$$F_{III} = \frac{K_{III}(x,y)\big|_{x=x,y=\pm b}}{\sigma_z^\infty\sqrt{\pi a}} = \sum_{l=1}^{2}\frac{1+\kappa_l}{4\mu_l\cosh\pi\varepsilon} \times \frac{1}{(1/\mu_1 + 1/\mu_2)}\sqrt{a^2-x^2}\sin\left(\varepsilon\ln(\frac{a-x}{a+x})\right)F_x. \quad (12b)$$

5.2 Convergence of numerical solutions

Convergence of numerical solutions when a/b=1, $\varepsilon = 0.02$, $\mu_2/\mu_1 = 1.5628$, $\nu_1 = 0.3$, $\nu_2 = 0.3$ is shown in Table 1,2 and 3. Here, in order to satisfy the boundary conditions, the least square regression method is applied to calculate $\alpha_i, \beta_i, \gamma_i$ to minimize the residual stress at collocation points considered on the mesh on the crack region. As shown in Tables 1, 2, 3 the present solutions show good convergence of the results.

5.3 Numerical analysis example

Tables 4 and 5 indicate values of F_I and F_{II} when the polynomial exponent $m = n = 8$, a/b=1, $\varepsilon = 0.02$ with varying Poisson ratio ν_1, ν_2 and stiffness ratio μ_1/μ_2. It should be noted that values of F_I and F_{II} are clearly independent of the values of μ_1/μ_2, ν_1,ν_2 under fixed values of a/b and ε. As shown in Table 5, at $x/a = 10/11$ the F_{II} values are slightly depending on μ_1/μ_2 and ν_1,ν_2. However, this may be due to the error including numerical solutions and the F_{II} values may be controlled by ε alone because the convergence in Table 1-3 becomes bad as $x/a \to 1$.

Here, the unknown coefficient $\alpha_i, \beta_i, \gamma_i$ in Eq. (8) varies depending on μ_1/μ_2, ν_1,ν_2

Table 1 Convergence of stress intensity factor F_I at $y=b$ for $\varepsilon = 0.02$, $\mu_2/\mu_1 = 1.5628$, $\nu_1 = 0.3$, $\nu_2 = 0.3$, a/b=1

x/a	0/11	1/11	2/11	3/11	4/11	5/11	6/11	7/11	8/11	9/11	10/11
m=n=4	0.7531	0.7512	0.7457	0.7364	0.7233	0.7059	0.6828	0.6517	0.6073	0.5385	0.4177
m=n=6	0.7524	0.7507	0.7456	0.7367	0.7237	0.7060	0.6826	0.6519	0.6098	0.5465	0.4329
m=n=8	0.7528	0.7511	0.7459	0.7369	0.7238	0.7058	0.6822	0.6514	0.6099	0.5490	0.4400

Table 2 Convergence of stress intensity factor F_{II} at $y=b$ for $\varepsilon = 0.02$, $\mu_2/\mu_1 = 1.5628$, $\nu_1 = 0.3$, $\nu_2 = 0.3$, a/b=1

x/a	0/11	1/11	2/11	3/11	4/11	5/11	6/11	7/11	8/11	9/11	10/11
m=n=4	0.0272	0.0271	0.0268	0.0264	0.0257	0.0248	0.0236	0.0221	0.0200	0.0171	0.0127
m=n=6	0.0273	0.0272	0.0270	0.0265	0.0259	0.0250	0.0238	0.0223	0.0203	0.0174	0.0131
m=n=8	0.0274	0.0273	0.0271	0.0266	0.0260	0.0251	0.0239	0.0224	0.0203	0.0176	0.0133

Table 3 Convergence of stress intensity factor F_{III} at $y=b$ for $\varepsilon = 0.02$, $\mu_2/\mu_1 = 1.5628$, $\nu_1 = 0.3$, $\nu_2 = 0.3$, a/b=1

x/a	0/11	1/11	2/11	3/11	4/11	5/11	6/11	7/11	8/11	9/11	10/11
m=n=4	0	0.0010	0.0021	0.0031	0.0042	0.0053	0.0065	0.0079	0.0094	0.0109	0.0120
m=n=6	0	0.0010	0.0020	0.0031	0.0041	0.0052	0.0064	0.0076	0.0091	0.0106	0.0120
m=n=8	0	0.0010	0.0020	0.0031	0.0041	0.0051	0.0063	0.0075	0.0089	0.0105	0.0120

Table 4 Stress intensity factor F_I at $y=b$ for a/b=1, $\varepsilon = 0.02$

ν_1	ν_2	μ_2/μ_1	0/11	1/11	2/11	3/11	4/11	5/11	6/11	7/11	8/11	9/11	10/11
0	0	1.2870	0.7528	0.7511	0.7459	0.7370	0.7238	0.7059	0.6822	0.6513	0.6099	0.5490	0.4400
0	0.1	1.0439	0.7528	0.7511	0.7459	0.7369	0.7238	0.7059	0.6822	0.6513	0.6099	0.5490	0.4400
0	0.2	0.8009	0.7528	0.7511	0.7459	0.7369	0.7238	0.7058	0.6822	0.6513	0.6099	0.5490	0.4400
0	0.3	0.5578	0.7528	0.7511	0.7459	0.7369	0.7238	0.7058	0.6822	0.6514	0.6099	0.5490	0.4400
0	0.4	0.3148	0.7528	0.7511	0.7459	0.7369	0.7238	0.7058	0.6822	0.6514	0.6099	0.5490	0.4400
0	0.5	0.0718	0.7527	0.7511	0.7459	0.7369	0.7238	0.7058	0.6822	0.6514	0.6099	0.5490	0.4400
0.1	0.1	1.3288	0.7528	0.7511	0.7459	0.7369	0.7238	0.7059	0.6822	0.6514	0.6099	0.5490	0.4400
0.1	0.2	1.0194	0.7528	0.7511	0.7459	0.7369	0.7238	0.7058	0.6822	0.6514	0.6099	0.5490	0.4400
0.1	0.3	0.7101	0.7528	0.7511	0.7459	0.7369	0.7238	0.7058	0.6822	0.6514	0.6099	0.5490	0.4400
0.1	0.4	0.4007	0.7528	0.7511	0.7459	0.7369	0.7238	0.7058	0.6822	0.6514	0.6099	0.5490	0.4400
0.1	0.5	0.0913	0.7527	0.7511	0.7459	0.7369	0.7238	0.7058	0.6822	0.6514	0.6099	0.5490	0.4400
0.2	0.2	1.4019	0.7528	0.7511	0.7459	0.7369	0.7238	0.7058	0.6822	0.6514	0.6099	0.5490	0.4400
0.2	0.3	0.9765	0.7528	0.7511	0.7459	0.7369	0.7238	0.7058	0.6822	0.6514	0.6099	0.5490	0.4400
0.2	0.4	0.5510	0.7528	0.7511	0.7459	0.7369	0.7238	0.7058	0.6822	0.6514	0.6099	0.5490	0.4400
0.2	0.5	0.1256	0.7527	0.7511	0.7459	0.7369	0.7238	0.7058	0.6822	0.6514	0.6099	0.5490	0.4400
0.3	0.3	1.5628	0.7528	0.7511	0.7459	0.7369	0.7238	0.7058	0.6822	0.6514	0.6099	0.5490	0.4400
0.3	0.4	0.8819	0.7528	0.7511	0.7459	0.7369	0.7238	0.7058	0.6822	0.6514	0.6099	0.5490	0.4400
0.3	0.5	0.2010	0.7527	0.7511	0.7459	0.7369	0.7238	0.7058	0.6822	0.6514	0.6099	0.5490	0.4400
0.4	0.4	2.2076	0.7527	0.7511	0.7459	0.7369	0.7238	0.7058	0.6822	0.6514	0.6099	0.5490	0.4400
0.4	0.5	0.5032	0.7527	0.7511	0.7459	0.7369	0.7238	0.7058	0.6822	0.6514	0.6099	0.5490	0.4400
0.45	0.5	2.0257	0.7527	0.7511	0.7459	0.7369	0.7328	0.7058	0.6822	0.6514	0.6099	0.5490	0.4400

Table 5 Stress intensity factor F_{II} at $y=b$ for a/b=1, $\varepsilon=0.02$

ν_1	ν_2	μ_2/μ_1	0/11	1/11	2/11	3/11	4/11	5/11	6/11	7/11	8/11	9/11	10/11
0	0	1.2870	0.0278	0.0277	0.0274	0.0269	0.0262	0.0253	0.0241	0.0224	0.0202	0.0171	0.0122
0	0.1	1.0439	0.0277	0.0277	0.0274	0.0269	0.0262	0.0253	0.0241	0.0224	0.0203	0.0172	0.0124
0	0.2	0.8009	0.0277	0.0276	0.0273	0.0268	0.0262	0.0252	0.0240	0.0224	0.0203	0.0173	0.0126
0	0.3	0.5578	0.0276	0.0275	0.0272	0.0268	0.0260	0.0252	0.0240	0.0224	0.0203	0.0174	0.0129
0	0.4	0.3148	0.0274	0.0273	0.0271	0.0266	0.0260	0.0251	0.0239	0.0224	0.0204	0.0176	0.0134
0	0.5	0.0718	0.0271	0.0270	0.0268	0.0264	0.0258	0.0250	0.0238	0.0223	0.0204	0.0178	0.0141
0.1	0.1	1.3288	0.0277	0.0276	0.0273	0.0268	0.0262	0.0252	0.0240	0.0224	0.0203	0.0173	0.0126
0.1	0.2	1.0194	0.0276	0.0275	0.0273	0.0268	0.0261	0.0252	0.0240	0.0224	0.0203	0.0173	0.0127
0.1	0.3	0.7101	0.0275	0.0274	0.0272	0.0267	0.0261	0.0252	0.0240	0.0224	0.0203	0.0174	0.0130
0.1	0.4	0.4007	0.0274	0.0273	0.0270	0.0266	0.0260	0.0251	0.0239	0.0224	0.0204	0.0176	0.0134
0.1	0.5	0.0913	0.0271	0.0270	0.0268	0.0264	0.0258	0.0250	0.0238	0.0223	0.0204	0.0178	0.0141
0.2	0.2	1.4019	0.0275	0.0274	0.0272	0.0267	0.0261	0.0252	0.0240	0.0224	0.0203	0.0174	0.0129
0.2	0.3	0.9765	0.0275	0.0274	0.0271	0.0267	0.0260	0.0251	0.0240	0.0224	0.0204	0.0175	0.0131
0.2	0.4	0.5510	0.0273	0.0272	0.0270	0.0266	0.0260	0.0251	0.0239	0.0224	0.0204	0.0176	0.0135
0.2	0.5	0.1256	0.0271	0.0270	0.0268	0.0264	0.0258	0.0250	0.0238	0.0223	0.0203	0.0178	0.0141
0.3	0.3	1.5628	0.0274	0.0273	0.0271	0.0266	0.0260	0.0251	0.0239	0.0224	0.0204	0.0176	0.0134
0.3	0.4	0.8819	0.0273	0.0272	0.0270	0.0266	0.0259	0.0251	0.0239	0.0224	0.0204	0.0177	0.0136
0.3	0.5	0.2010	0.0271	0.0270	0.0268	0.0264	0.0258	0.0250	0.0238	0.0223	0.0204	0.0178	0.0141
0.4	0.4	2.2076	0.0272	0.0271	0.0269	0.0265	0.0259	0.0250	0.0239	0.0224	0.0204	0.0177	0.0138
0.4	0.5	0.5032	0.0271	0.0270	0.0268	0.0264	0.0258	0.0250	0.0238	0.0223	0.0204	0.0178	0.0141
0.45	05	2.0257	0.0271	0.0270	0.0268	0.0264	0.0258	0.0250	0.0238	0.0223	0.0204	0.0178	0.0141

Table 6 Stress intensity factor $F_{III}\times10^{-2}$ at $y=b$ for a/b=1, $\varepsilon=0.02$

ν_1	ν_2	μ_2/μ_1	0/11	1/11	2/11	3/11	4/11	5/11	6/11	7/11	8/11	9/11	10/11
0.3	0.3	1.5628	0	0.1010	0.2028	0.3061	0.4115	0.5199	0.6331	0.7545	0.8913	1.051	1.204
0.0	0.5	0.0718	0	0.0869	0.1746	0.2637	0.3550	0.4500	0.5517	0.6662	0.8011	0.9592	1.099
0.0	0.0	1.2870	0	0.1204	0.2415	0.3641	0.4884	0.6141	0.7400	0.8667	1.000	1.156	1.328

even under the same value of ε. However, F_I, F_{II} are independent of μ_1/μ_2, ν_1,ν_2 although they are expressed as a combination of those coefficients. Therefore it seems difficult to prove that F_I, F_{II} are the functions of ε from Eqs. (1)-(12) theoretically.

As shown in Table 6, the maximum value of mode III stress intensity factor F_{III} appears at near the corner of the interface crack and always takes a small value in the range $F_{III\,\max}\le10^{-4}\times F_{I\,\max}$ and $F_{III\,\max}\le0.5\times F_{II\,\max}$. Currently it is not clear that F_{III} is controlled by ε alone or not.

6. Conclusion

In this paper, numerical solutions of hypersingular integral equations for a 3D interfacial crack were considered when the crack shape is rectangular as an example. The conclusions can be summarized as follows:

(1) The 3D interfacial crack problems can be expressed as a system of hypersingular intergro-differential equations on the idea of the body force method. Then, unknown functions are approximated by the product of the fundamental density functions and polynomials. The fundamental density functions are chosen to express peculiar oscillation singular stress field exactly considering 2D solutions. The stress intensity factors are determined from the values of unknown functions directly. The present method shows good convergence as shown in Tables 1-3.

(2) The present calculations shows that the stress intensity factors K_I, K_{II} of 3D interfacial cracks are determined by the bimaterial constant ε alone as shown in Tables 4 and 5.

(3) For the rectangular interfacial crack under tension the maximum value of K_{III} appears at a point which is very close to the corner of the rectangle. The F_{III} values are smaller and in the range $F_{III\,\max}\le10^{-2}\times F_{I\,\max}$ and $F_{III\,\max}\le0.5\times F_{II\,\max}$ (see Table 6).

References

(1) Salganik, R.L., The Brittle Fracture of Cemented Bodies, *Prikladnaia metematica i mekhanika,* Vol. 27, (1963), pp. 957-962
(2) Erdogan, F., Stresses Distribution in a Non-homogeneous Elastic Plane with Crack, *Transaction of the ASME, Journal of Applied Mechanics,.,* Vol. 30, (1963), pp. 232-236
(3) England, A.H., A Crack between Dissimilar Media, *Transaction of the ASME, Journal of Applied Mechanics,* Vol. 32 , (1965), pp. 400-402
(4) Rice, J. R. and Sih, G. C., Plane Problems of Cracks in Dissimilar Media. *Transaction of the ASME, Journal of Applied Mechanics,* Vol. 32, (1965), pp. 418-423
(5) Comninou, M., The Interface Crack. *Transaction of the ASME, Journal of Applied Mechanics,* Vol. 44, (1977), pp.631-636
(6) Noda, N-A and Oda, K., Interaction Effect of Stress Intensity Factors for any Number of Collinear Interface Cracks, *International Journal of Fracture,* Vol. 84, (1997), pp.117-128
(7) Willis, J.R., Fracture Mechanics of Interfacial Crack, *Journal of the Mechanics and Physics of solids,* Vol. 19, (1971) ,pp.353-368
(8) Tucker, M. O., In Two-phase Solids under Longitudinal Shear Loading, *International Journal of Fracture,* Vol.10, (1974), pp. 323-336
(9) England, F. and Gupta,G.D., Bonded Wedges with an Interface Crack under Anti-plane Shear Loading, *International Journal of Fracture,* Vol.11, (1975), pp.593-593
(10) Willis, J.R., The Penny-Shaped Crack on an Interface, *Journal of Mechanics Applied Mathmatica*， Vol. 25, (1972), pp.367-385
(11) Mossakovski, V.I. , and Rybka, M.T., Generalization of the Griffith-Sneddon Criterion for the Case of a Non-homogeneous Body, *Prikladnaia metematica i mekhanika,* Vol. 28, (1964), pp.1061-1069
(12) England, F., Stress Distribution in Bonded Dissimilar Materials Containing Circular or Ring-Shaped Cavities, *Transaction of the ASME, Journal of Applied Mechanics, Series E*, Vol. 32, (1965), pp.829-836
(13) (13) Kassir, M.K., and Bregman, A. M., The Stress Intensity Factor for a Penny-Shaped Crack between Two Dissimilar Materials, *Transaction of the ASME, Journal of Applied Mechanics, Series E*, Vol. 39, (1972), pp.308-310
(14) Lowengrub, M. and Sneddon,I. N., The Effect of Internal Pressure on a Penny-Shaped Crack at the Interface of Two Bonded Dissimilar Elastic Half-Spaces, *International Journal of Engineering Science*, Vol. 12, (1974), pp.387-396
(15) Keer, L. M. Chen, S. H. and Comninou,M., The Interface Penny-Shaped Crack Reconsidered, *International Journal of Engineering Science*, Vol.16, (1978), pp. 765-772
(16) Shibuya, T., Koizumi, T., Iwamoto, T., Stress Analysis of the Vicinity of an Elliptical Crack at the Interface of Two Bonded Half-Spaces, *JSME International Journal, Series A,* Vol.32, (1989), pp.485-491
(17) Yuuki, R., Cao, X. F., Boundary Element Analysis to Stress Intensity Factor of Interface Crack, *Transaction of the Japan Society of Mechanical Engineering, Series A,* (in Japanese) No.55-510,(1989）, pp.340-347
(18) Takakuda, K., Shibuya, T., and Koizumi, T., Stress Analysis for biomaterial with an Interface Crack, *In: Prelim. Proc. 55th Annual Meeting of Japan Soc. Mech. Engrs.,* (in Japanese) No. 780-3, (1978), pp.167-169
(19) Noda, N.A., Kagita, M., and Chen, M,C., Analysis of Stress Intensity Factors of a Ring-Shaped Interface Crack, *International Journal of Solids and Structures*, Vol.40, No.24, (2003), pp.6577-6592
(20) Qing W. and Noda, N.A.,Variation of Stress Intensity Factors along the Front of 3D Rectangular Crack by Using a Singular Integral Equation Method, *International Journal of Fracture*, Vol. 108,(2001), pp.119-131
(21) Qin T.Y. and Noda, N.A., Three-Dimensional Crack Problem Analysis Using Boundary Element Method ｗｈｉｔ Finite-part Integrals, *International Journal of Fracture,* Vol.84,(1997), pp.191-202
(22) Qin T.Y. and Noda, N. A., Stress Intensity Factors of Rectangular Crack Meeting a Bimateral Interface, *International Journal of Solids and Structures,* Vol. 40,(2003),

pp.2473-2486
(23) Chen M.C. Noda, N.A. and Tang, R.J.,, Application of Finite-part Integrals to Planar Interfacial Fracture Problems in Three Dimensional Bimaterials, *Journal of Applied Mechanics,* Vol.66, (1999), pp.885-890